Supporting Information

Scalable Chitosan-Graphene Oxide Membranes: The Effect of GO Size on Properties and Cross-Flow Filtration Performance

Mojtaba Abolhassani,[a] Chris S. Griggs,[b] Luke A. Gurtowski,[b] Jose A. Mattei-Sosa,[b] Michelle Nevins,[b,c] Victor F. Medina,[b] Timothy A. Morgan,[d] Lauren F. Greenlee[a*]

[a] Ralph E. Martin Department of Chemical Engineering, 3202 Bell Engineering Center, University of Arkansas, Fayetteville, AR 72701, USA

[b] U.S. Army Engineer Research Development Center, 3909 Halls Ferry Road, Vicksburg, MS 39180, USA

[c] State University of New York at Stony Brook, Stony Brook, NY 11794, USA

[d] Institute for Nanoscience and Engineering, 731 W Dickson St., University of Arkansas, Fayetteville, AR 72701, USA

*Corresponding Author, Email: greenlee@uark.edu

Author Information:

The author email addresses are as follows: mabolhas@email.uark.edu, Chris.S.Griggs@usace.army.mil, Luke.A.Gurtowski@usace.army.mil, Jose.A.Mattei-Sosa@usace.army.mil, michelle8nevins@gmail.com, Victor.F.Medina@usace.army.mil, tamorga@uark.edu, greenlee@uark.edu

Supporting Information

Cross-Flow Filtration Setup

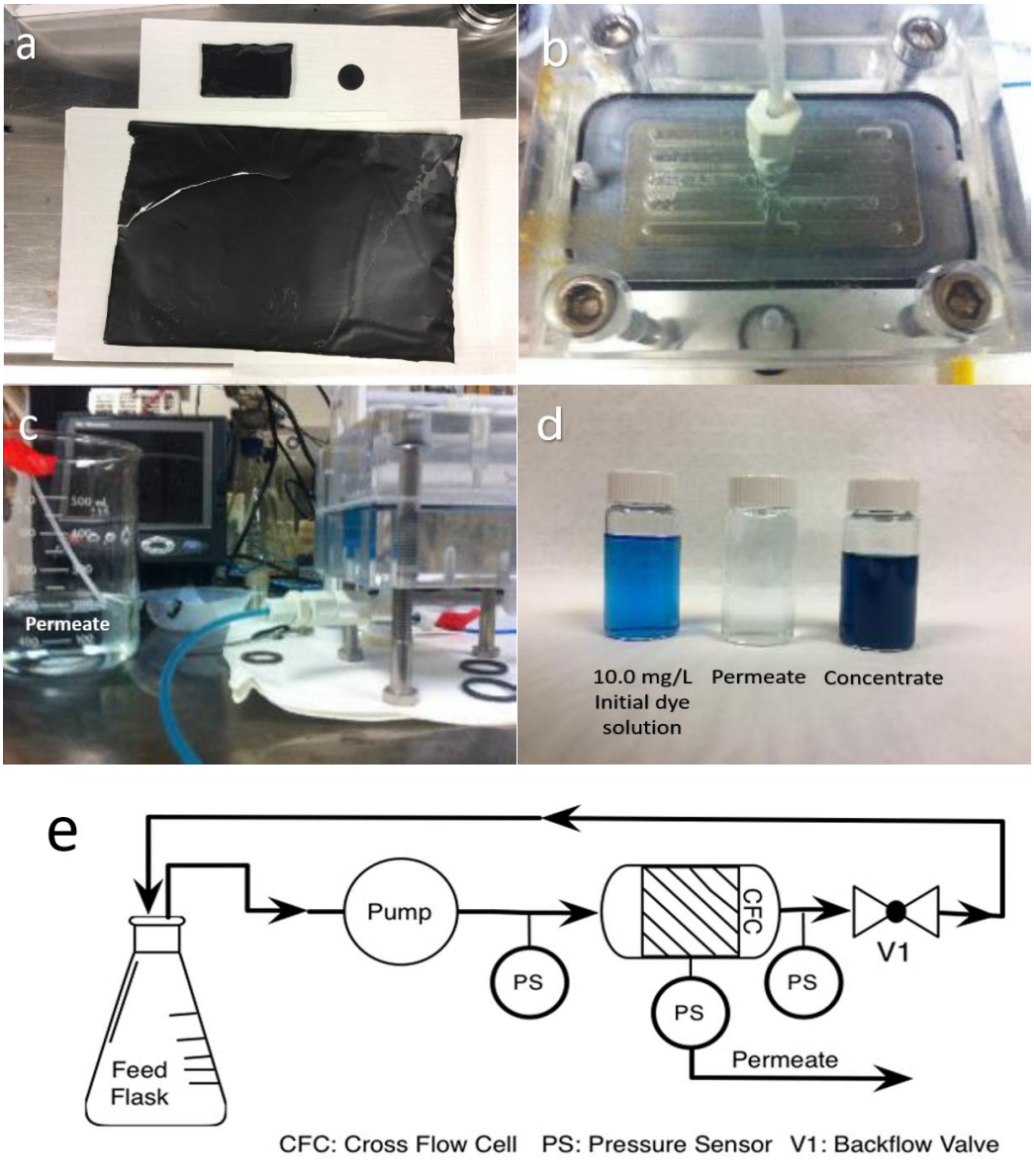

Figure S1. (a) Flat sheet CSGO membrane cast from CSGO solution evaporation. (b) Cross flow membrane cell used for performance testing. (c) Digital image of collected permeate and retentate tube that returns retentate to the feed flask. (d) Collected samples for methylene blue analysis displaying an observable difference in dye concentration in the feed solution, permeate, and concentrate (retentate). (e) Schematic diagram of the cross flow membrane experimental setup.

Additional Characterization Data

Membrane Thickness

Representative cross-sectional SEM images are shown in Figure S2 with measurements of membrane thickness. Membrane thickness measurements were taken on at least 3 different membrane samples and the average and standard deviation for each membrane type are reported in the main article. All membranes were prepared by freeze-fracturing after exposure to liquid nitrogen.

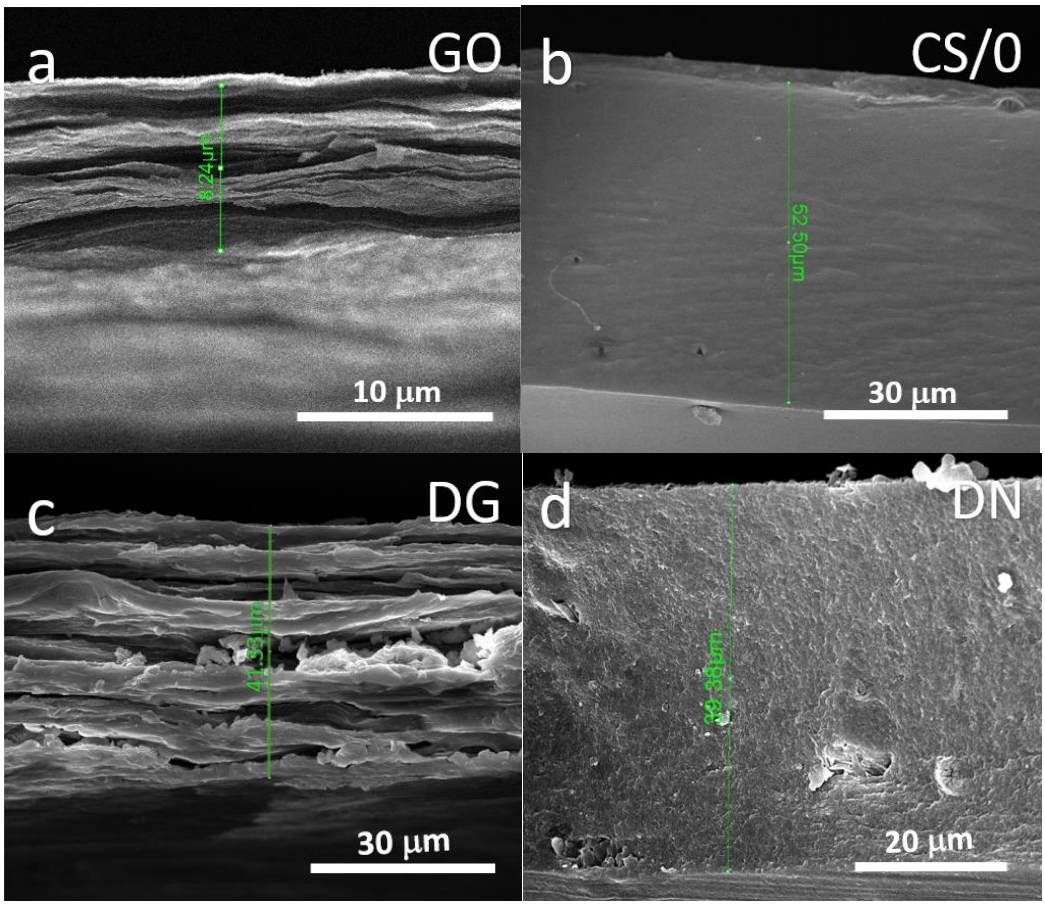

Figure S2. SEM cross-section images of (a) GO, (b) CS/0, (c) DG-CSGO, and (d) DN-CSGO. The thickness of the membranes are 8.2, 52.5, 41.3, and 39.4 µm for GO, CS/0, DG-CSGO, and DN-CSGO, respectively, as measured on representative membrane cross-sections.

XPS Results

In addition to the C 1s and N 1s spectra, the GO membrane was also analyzed for the Al 2p region (Figure S3). Based on previously reported results,[1] it was expected that the porous anodized aluminum oxide filter would release Al^{3+} during formation of the GO membrane, resulting in Al^{3+} cross-linked within the GO membrane. This incorporation of Al^{3+} into the GO membrane structure has been shown to be key to enabling membrane mechanical integrity where the membrane stiffness can be increased to 340% using AAO filters.[1] It has also been suggested that the Al^{3+} concentration within the GO membrane may vary through the thickness of the membrane due to the location of the AAO filter on only the bottom side of the GO membrane during membrane fabrication.[1] The XPS Al 2p spectra obtained for the top and bottom surfaces of the GO membrane are compared in Figure S3, where the Al/C atomic ratio for the top and bottom surfaces of the GO membrane was ~ 1% and 2%, respectively. This result indicates Al^{3+} is present in all the layers throughout the thickness of the GO membrane but that the concentration of Al^{3+} increases from the top to the bottom of the membrane. The measured Al/C ratios were different because the bottom layers of the GO membrane were in contact with the AAO filter more than the top layers during the 72 h filtration. If a general mechanism of diffusion is assumed for Al^{3+} incorporation into the GO membrane, where Al^{3+} dissolution from the AAO filter and through the GO membrane is slow compared to the overall membrane fabrication time, a concentration gradient of Al^{3+} through the membrane would exist. This concentration gradient would thus result in a measured decrease in Al^{3+} concentration from the bottom to the top of the fabricated membrane.

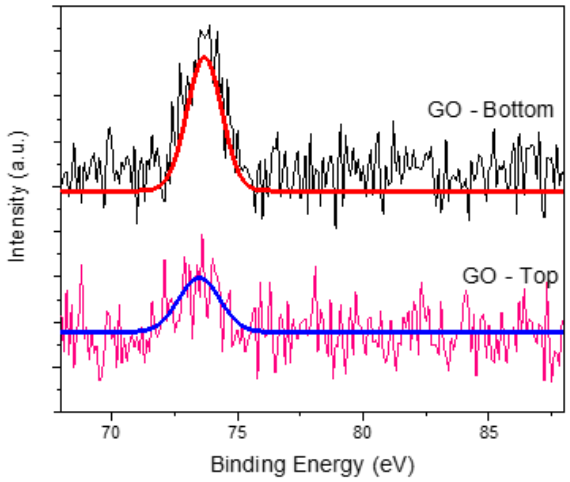

Figure S3. XPS Al 2p spectra of bottom and top side of GO membrane.

EDX Results

As EDX is considered to be semi-quantitative, EDX results are used to support results obtained by XPS and are used as relative measurements within the sample set of membranes reported herein, rather than quantitative, absolute measurements. The GO membrane sample contained 60.8% carbon and 38.0% oxygen, which are correlated to the carbon ring backbone and oxygen-containing functional groups of the membrane. The 0.5% sulfur in the GO sample is likely due to the residual sulfur from H_2SO_4 used in GO preparation from graphene. The Al^{3+} released from the AAO filter was also observed in the GO membrane. In comparison with the top side of the GO, the bottom side shows approximately the same amount of C, O, and S; this result is expected since EDX is a bulk characterization technique, whereas XPS is a surface sensitive technique, probing only the first 5-10 nm of the membrane sample. The EDX results for the CS/0 membrane indicate an atomic distribution of 62.0% as C, 27.5% as O, and 10.6% as N in the membrane. The CSGO membranes also show ~8% N because of the amine groups of CS. Overall, the EDX results confirm and support results presented in Figure 3 and Table 1 for XPS analysis.

Table S1. EDX results of the four membrane samples.

Element	GO Top (%)	GO Bottom (%)	DG-CSGO (%)	DN-CSGO (%)	CS/0 (%)
C	60.8	59.2	51.9	53.4	62.0
O	38.0	39.1	39.7	38.7	27.5
N	0	0	8.1	7.9	10.6
S	0.5	0.5	0	0	0
Al	0.7	1.2	0	0	0

FTIR Results

The presence of amide I and amide II bands are shown in the IR spectrum of the CS/0 membrane with two peaks at 1640 and 1542 cm^{-1}, respectively. The peaks at 1018 and 1152 cm^{-1} confirm the presence of primary (C6-OH) and secondary (C3-OH) alcoholic groups, respectively. Broad peaks in the range of 2500 to 3500 cm^{-1} indicate N–H (amino group) and O–H stretching. The FTIR spectrum of the GO membrane also consists of several peaks. The four main peaks at 985, 1085, 1618, 1722 cm^{-1} are related to C-O-C bonds of epoxy, C-OH, C=C stretching mode of the sp2 carbon skeletal network, and C=O bonds, respectively. The spectrum for CSGO samples shows that typical peaks of the functional groups presented in the CS/0 membrane are also observed in the CSGO composite membranes. The peaks at around 1648 cm^{-1} and 1550 cm^{-1} correspond to C=O and N-H stretching. The intensity of the peaks decreases in the CSGO spectra, in comparison with pure CS. Moreover, some of the peaks, such as the amide group C=O bond, are shifted. The interaction of negative charge on GO surface and polycationic CS, as well as hydrogen bonding, may be responsible for these changes. The broad peaks in the range of 2500 to 3500 cm^{-1} are associated with the OH groups in GO and amine stretch from the CSGO mixture.

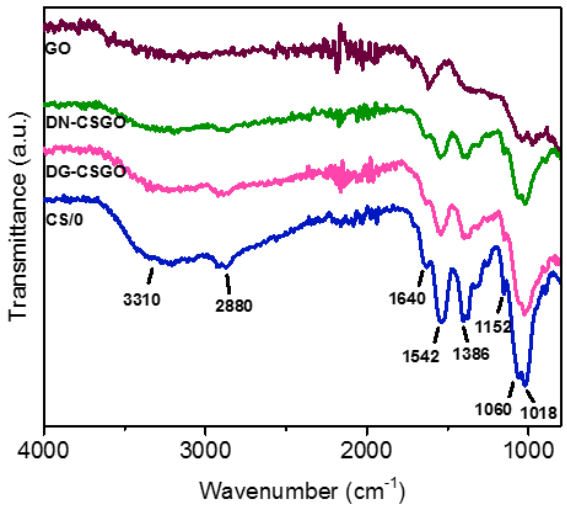

Figure S4. FTIR spectra of CS/0, GO, DG-CSGO, and DN-CSGO membranes.

XRD Results

For this set of measurements, the membranes were soaked in purified water for 30 min and then analyzed by XRD. The resulting XRD diffraction patterns are compared for both the dry and wet states in Figure S4. The characteristic XRD peak of synthesized GO is located at $2\theta=10.54^{o}$ in the dry membrane in Fig 6a. The Bragg equation was used to obtain a d-spacing of 8.38 Å for the dry membrane. This diffraction peak for GO shifted slightly to the left in the wet state, which demonstrates a slight increase in interlayer spacing of the GO membrane upon wetting; the intensity of the diffraction peak remained the same. The d-spacing of the wet membrane was calculated as 8.52 Å for $2\theta=10.37^{o}$. In stark contrast to the GO membrane, the diffraction peaks for both of the CSGO membranes disappeared in the wetted state, indicating a complete loss of crystallinity and structural order upon wetting. As expected, the Al^{3+} cross-linked GO, which was shown by XPS and EDX to contain a small amount of Al, retains the lamellar structure of the GO membrane once wetted.[1] In the composite CSGO membranes, the

loss of peaks suggests that the interactions between CS and GO were based on electrostatic and hydrogen bonding and that these interactions are not strong enough to retain the crystalline structure and order of the dry membrane once wetted. This result is likely to have implications for the long-term stability of the composite CSGO membranes during water filtration and will need to be addressed in future iterations of materials development.

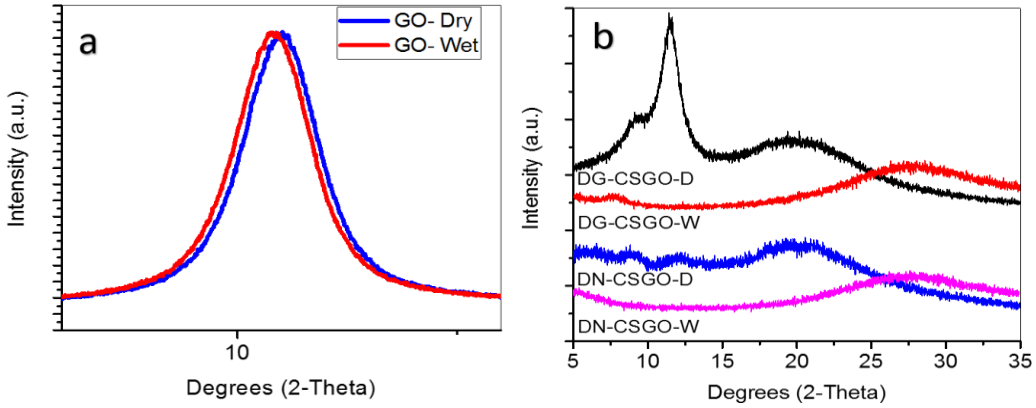

Figure S5. XRD patterns of (a) GO, and (b) DG-CSGO and DN-CSGO membranes in wet and dry states.

Tensile Test Results

Tensile testing (Figure S6) was used to study the mechanical behavior of the CS/0 and CSGO membranes. Good dispersion of GO particles into the CS matrix lead to proper load transfer from CS matrix to GO sheets. The mechanical properties of the composite increase because of the large aspect ratio of the GO sheets and also load transferring from CS matrix to GO sheets.[2-3] While at the low GO content (less than 6%) in CS matrix a good dispersion of GO particles and then improving the mechanical properties of the composites is observed, further increasing the GO content result in aggregation and defects at the composites and so tensile strength would be decreased.[2, 4-5] Although in a few papers, good dispersion and mechanical properties is achieved at high level of GO particles into the CS.[6] In this paper, the DG- and DN-CSGO composites

contain 17% GO were tested. While the Young's modulus of the CSGO membranes is approximately same as the CS/0, the ultimate tensile stress for CSGO membranes is less than CS/0, which may be a result of the high GO content. It is apparent in Figure S5 that the CSGO composite with nano GO particles has larger elongation at the break point in comparison with CS/0. DG-CSGO composite has different behavior from DN-CSGO. The elongation of DG-CSGO membrane is not only lower that DN-CSGO but also lower than CS/0. The presence of defects and displacement of the DG particles in loading may be the reason for low elongation at the break point for this membrane.

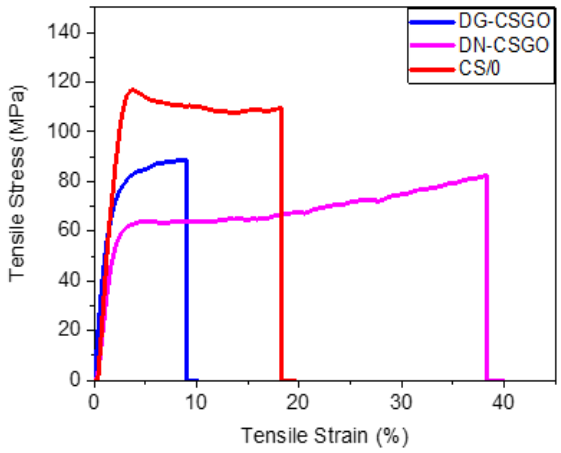

Figure S6. Stress–strain curves of CS/0, DG-CSGO, and DN-CSGO.

Additional Performance Data

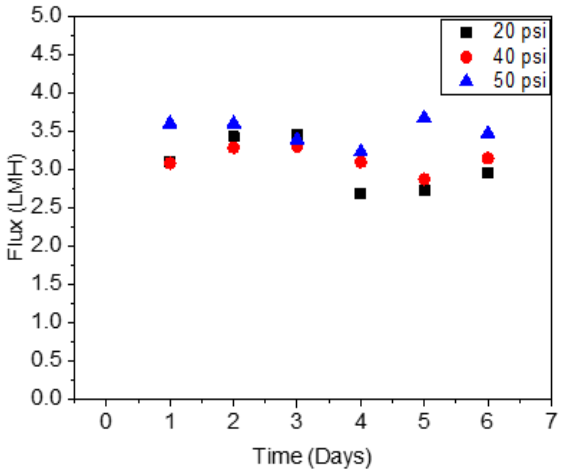

Figure S7. Pure water flux performance over time for a range of applied hydrostatic pressures. Membrane tested was a DG-CSGO membrane at a 1.8 x 10^{-3} m/s cross-flow velocity.

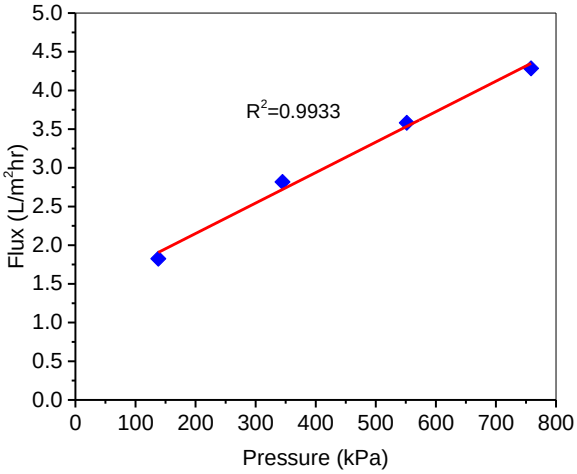

Figure S8. Flux vs. Pressure of DG-CSGO composite membrane.

Additional Characterization for GO

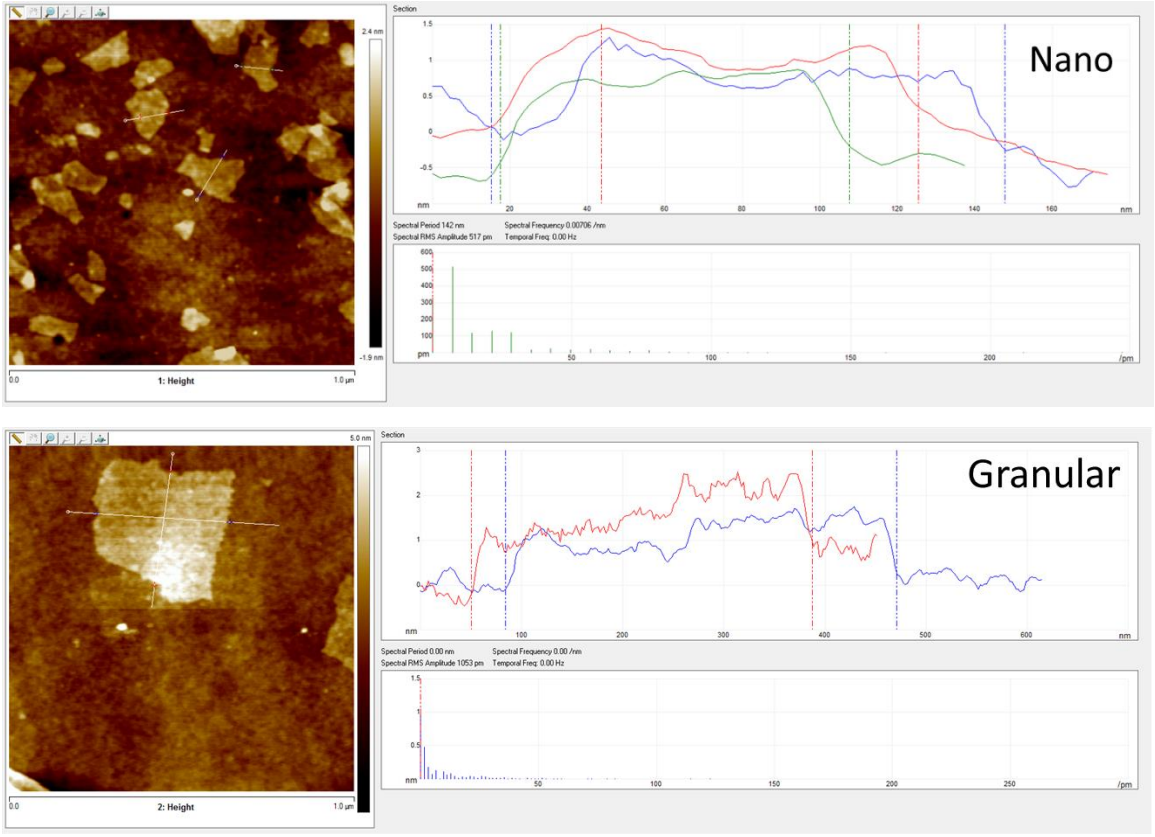

Figure S9. Tapping mode AFM images for single layer nano and granular GO particles on silicon wafer.

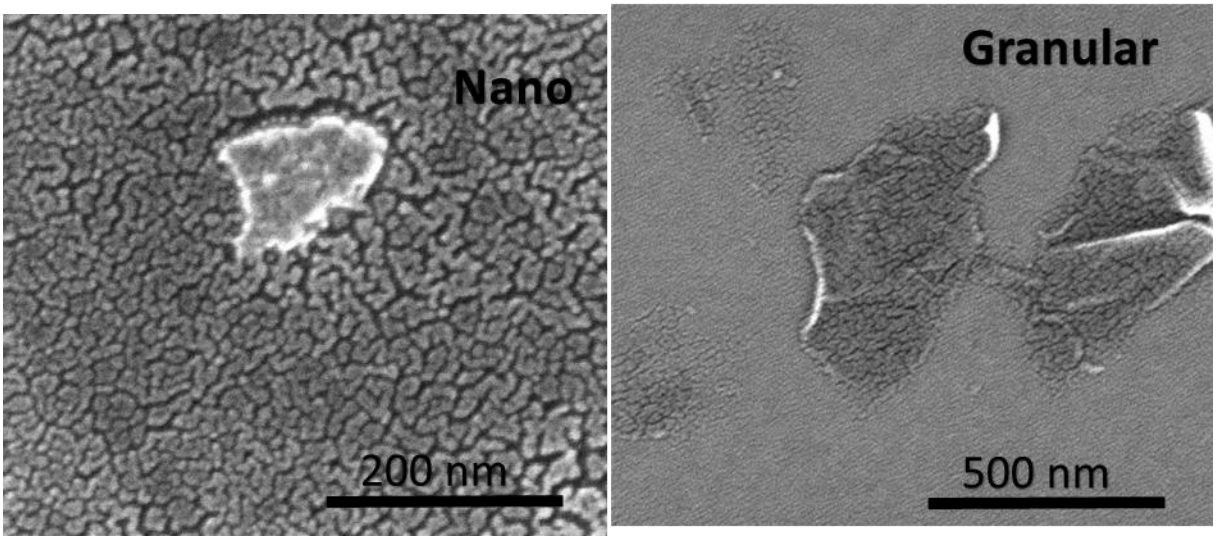

Figure S10. SEM images for nano and granular GO particles.

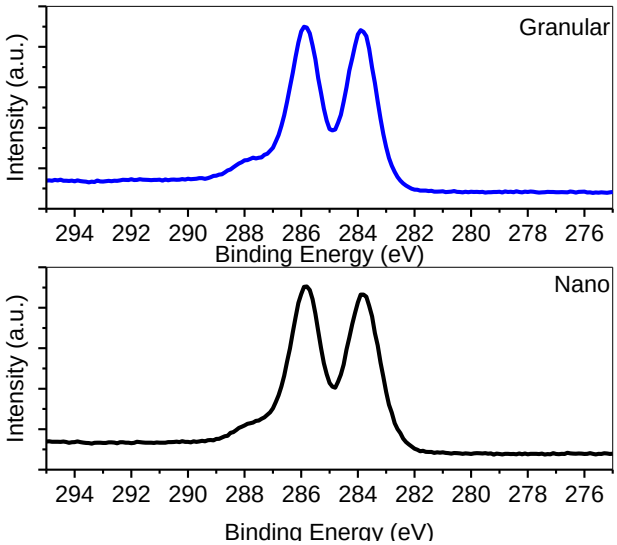

Figure S11. XPS C 1s spectra of nano and granular GO particles.

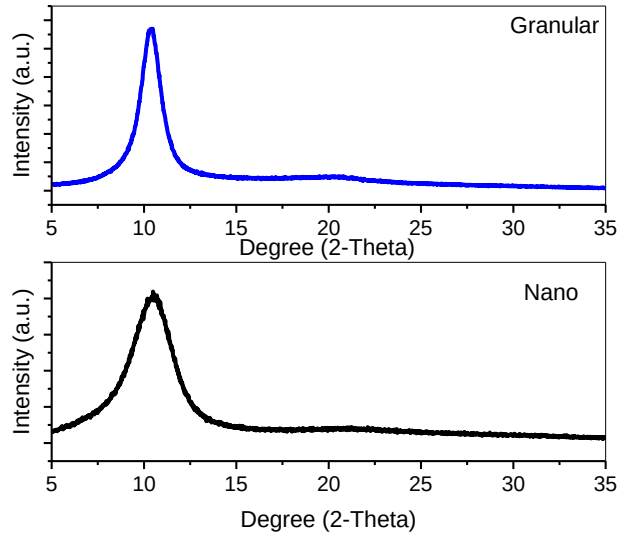

Figure S12. XRD patterns of nano and granular GO particles.

References

(1) Yeh, C.-N.; Raidongia, K.; Shao, J.; Yang, Q.-H.; Huang, J., On the origin of the stability of graphene oxide membranes in water. *Nat. Chem.* **2015,** *7* (2), 166-170.

(2) Pandele, A. M.; Dinescu, S.; Costache, M.; Vasile, E.; Obreja, C.; Iovu, H.; Ionita, M., Preparation and in vitro, bulk, and surface investigation of chitosan/graphene oxide composite films. *Polym. Comp.* **2013,** *34* (12), 2116-2124.

(3) Li, Y.; Sun, J.; Du, Q.; Zhang, L.; Yang, X.; Wu, S.; Xia, Y.; Wang, Z.; Xia, L.; Cao, A., Mechanical and dye adsorption properties of graphene oxide/chitosan composite fibers prepared by wet spinning. *Carbohyd. Polym.* **2014,** *102*, 755-761.

(4) Pandele, A. M.; Ionita, M.; Crica, L.; Dinescu, S.; Costache, M.; Iovu, H., Synthesis, characterization, and in vitro studies of graphene oxide/chitosan–polyvinyl alcohol films. *Carbohyd. Polym.* **2014,** *102*, 813-820.

(5) Justin, R.; Chen, B., Characterisation and drug release performance of biodegradable chitosan–graphene oxide nanocomposites. *Carbohyd. Polym.* **2014,** *103*, 70-80.

(6) Han, D.; Yan, L.; Chen, W.; Li, W., Preparation of chitosan/graphene oxide composite film with enhanced mechanical strength in the wet state. *Carbohyd. Polym.* **2011,** *83* (2), 653-658.